Article
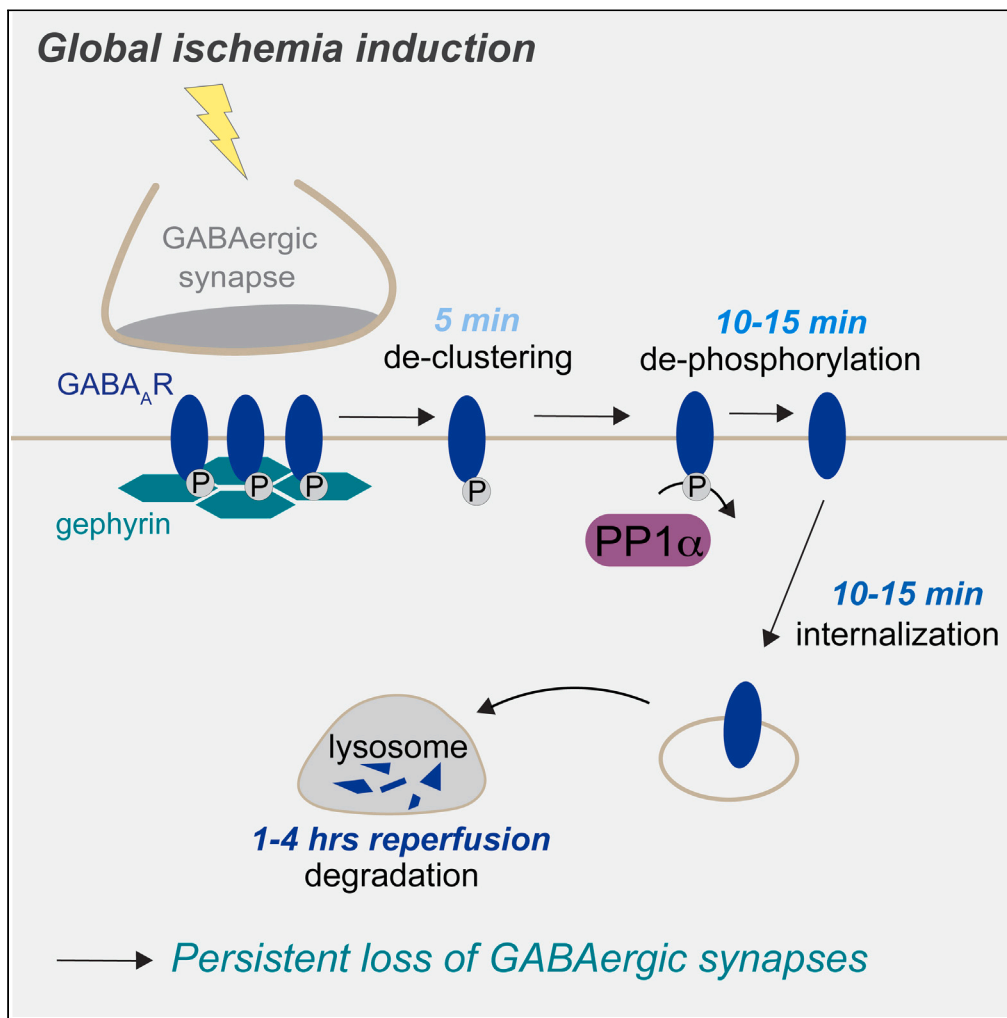
Distinct mechanisms drive sequential internalization and degradation of GABA$_A$Rs during global ischemia and reperfusion injury

Joshua D. Garcia, Sarah E. Wolfe, Amber R. Stewart, ..., Mayra Bueno Guerrero, Nidia Quillinan, Katharine R. Smith

katharine.r.smith@cuanschutz.edu

Highlights

Global ischemia initiates a sequential trafficking itinerary for GABA$_A$Rs

GABA$_A$Rs are dispersed from synapses and PP1α activity drives their surface removal

During reperfusion, GABA$_A$Rs are sorted to lysosomes for degradation

Together, these steps underly persistent loss of GABA$_A$Rs from synapses in ischemia

Article

Distinct mechanisms drive sequential internalization and degradation of GABA_ARs during global ischemia and reperfusion injury

Joshua D. Garcia,[1] Sarah E. Wolfe,[1] Amber R. Stewart,[1] Erika Tiemeier,[2] Sara E. Gookin,[1] Mayra Bueno Guerrero,[1] Nidia Quillinan,[2] and Katharine R. Smith[1,3,*]

SUMMARY

Synaptic inhibition is critical for controlling neuronal excitability and function. During global cerebral ischemia (GCI), inhibitory synapses are rapidly eliminated, causing hyper-excitability which contributes to cell-death and the pathophysiology of disease. Sequential disassembly of inhibitory synapses begins within minutes of ischemia onset: GABA_ARs are rapidly trafficked away from the synapse, the gephyrin scaffold is removed, followed by loss of the presynaptic terminal. GABA_ARs are endocytosed during GCI, but how this process accompanies synapse disassembly remains unclear. Here, we define the precise trafficking itinerary of GABA_ARs during the initial stages of GCI, placing them in the context of rapid synapse elimination. Ischemia-induced GABA_AR internalization quickly follows their initial dispersal from the synapse, and is controlled by PP1α signaling. During reperfusion injury, GABA_ARs are then trafficked to lysosomes for degradation, leading to permanent removal of synaptic GABA_ARs and contributing to the profound reduction in synaptic inhibition observed hours following ischemia onset.

INTRODUCTION

GABAergic inhibitory synapses mediate synaptic inhibition in the central nervous system, with key roles controlling neuronal and ensemble firing, excitatory/inhibitory (E/I) balance and synaptic plasticity.[1,2] As such, disruptions to inhibitory synapse function and plasticity can lead to impaired circuit function and is thought to contribute to the pathology of numerous neurological disorders including epilepsy, ischemia, autism spectrum disorders and schizophrenia.[3–5] At the inhibitory post-synaptic site, γ-aminobutyric acid (GABA) type A receptors (GABA_ARs) are clustered opposite presynaptic terminals where they mediate phasic inhibition. This post-synaptic receptor clustering is primarily governed by the inhibitory scaffold, gephyrin, along with myriad other proteins that make up the inhibitory post-synaptic domain.[6,7] The number of GABA_ARs at the synaptic site is a robust determinant of synaptic strength,[8] which is dynamically regulated during synaptic plasticity to strengthen or reduce inhibition in response to stimulation.[2,6,9] One way this is accomplished is through the trafficking of GABA_ARs to and from the synapse, via lateral diffusion, endocytosis, recycling, and degradation pathways, thereby enabling the highly regulated tuning of inhibitory synaptic strength.[6]

The disruption of E/I balance due to aberrant GABA_AR trafficking is thought to contribute to the pathology of multiple diseases including acute excitotoxic brain disorders such as global cerebral ischemia (GCI) and epilepsy.[4,10] The oxygen and glucose deprivation (OGD) produced by these excitotoxic insults, leads to the endocytosis of surface GABA_ARs and the persistent downregulation of GABAergic synapses and synaptic inhibition.[4,11,12] This drives cell and circuit hyper-excitability which contributes to delayed cell-death and sustained functional deficits in surviving neurons.[4,13–15] Although impairments in synaptic inhibition have been well-studied hours to days following the excitotoxic insult, far less attention has been paid to understanding the immediate molecular processes that drive inhibitory synaptic dysfunction during the onset of disease and immediate reperfusion phase (when oxygen and glucose are restored). Our recent work showed that GCI initiates a sequence of precisely-timed molecular events that result in the elimination of entire inhibitory synaptic structures, both *in vitro* and *in vivo*.[14] Immediately following OGD onset, activation of the phosphatase, calcineurin (CaN), causes rapid dispersal of GABA_ARs from synapses. This is quickly followed by cleavage and removal of the gephyrin scaffold by the protease calpain at ~15 min (Figure 1A), and loss of the presynaptic terminal at later time-points.[14] Thus, we have begun to provide a temporal and mechanistic framework for inhibitory synapse disassembly during pathogenic excitotoxicity. However, the precise
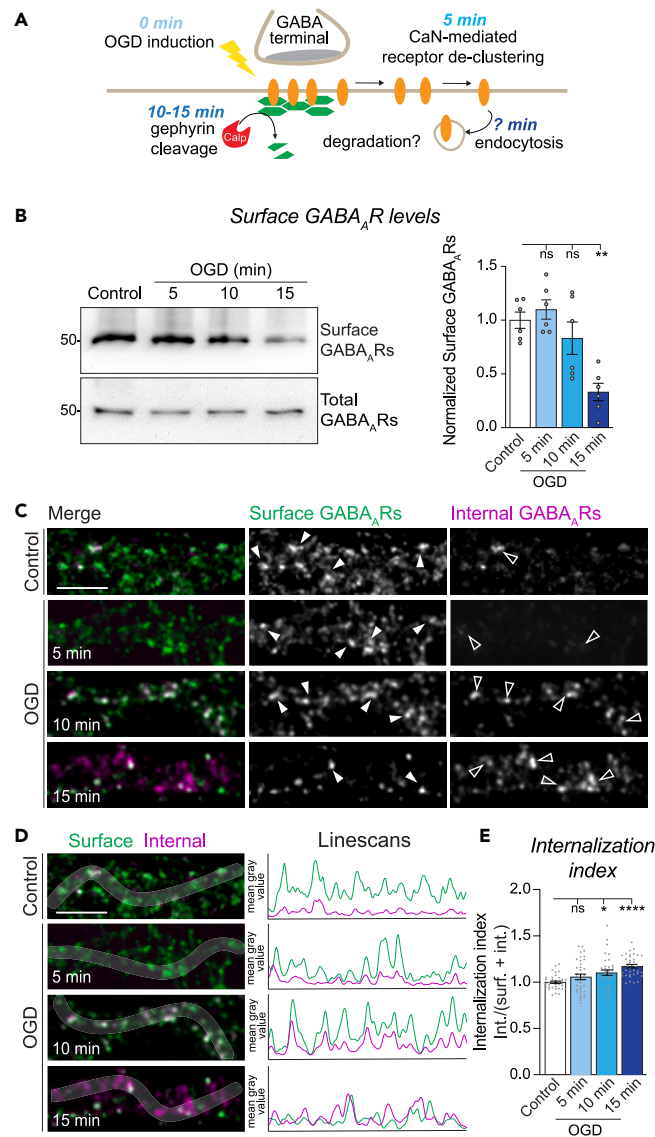
Figure 1. The temporal dynamics of GABA$_A$R internalization during OGD

(A) Schematic depicting the signaling events involved in GABAergic synapse disassembly following OGD onset. GABA$_A$Rs are dispersed from synaptic sites within 5 min, a process controlled by calcineurin (CaN). At 10 min, gephyrin is removed from synapses by calpain-dependent cleavage of the scaffold. Temporal kinetics of GABA$_A$R trafficking during OGD and subsequent reperfusion remain uncharacterized.

(B) Surface biotinylation of hippocampal neurons treated to an OGD time course at increasing 5 min intervals. Bar graphs show GABA$_A$R-α1 surface levels normalized to total levels (10% input), n = 6 independent experiments.

(C) Representative confocal images of dendritic segments from hippocampal neurons live-labeled for GABA$_A$R-γ2 and treated to an OGD time-course at increasing 5 min intervals. Arrows indicate high GABA$_A$R immunofluorescence peaks for surface (green) or internalized receptors (magenta). Filled arrowheads = surface GABA$_A$R clusters, open arrowheads = internalized GABA$_A$Rs. Scale = 5 µm.

(D) Example line scans represent the mean fluorescence intensity for each condition across the dendritic length (from left to right) for surface (green) or internalized (magenta) receptor pools. Grayed out line in merge image depicts path of line-scan. Scale = 5 µm.

(E) Quantification of the internalization index (ratio of the internalized immunofluorescence (IF)/(surface IF + internalized IF), n = 36 neurons. Values represent mean ± SEM. *p ≤ 0.05, **p < 0.01,****p < 0.0001, one-way ANOVA, Bonferroni post hoc test (B, E).

trafficking fate of GABA$_A$Rs following their initial dispersal from the synapse, the temporal and mechanistic details of this process, and the long-term fate of GABA$_A$Rs during early reperfusion is not well laid out.

Here, we used *in vitro* and *in vivo* GCI models to investigate the trafficking of GABA$_A$Rs following their dispersal from synaptic sites, during the initial phases of the ischemic insult and throughout the reperfusion phase that follows. We found that GABA$_A$Rs are internalized at ~15 min following ischemia-induction, a process that is controlled by the phosphatase PP1α and the phosphorylation state of the
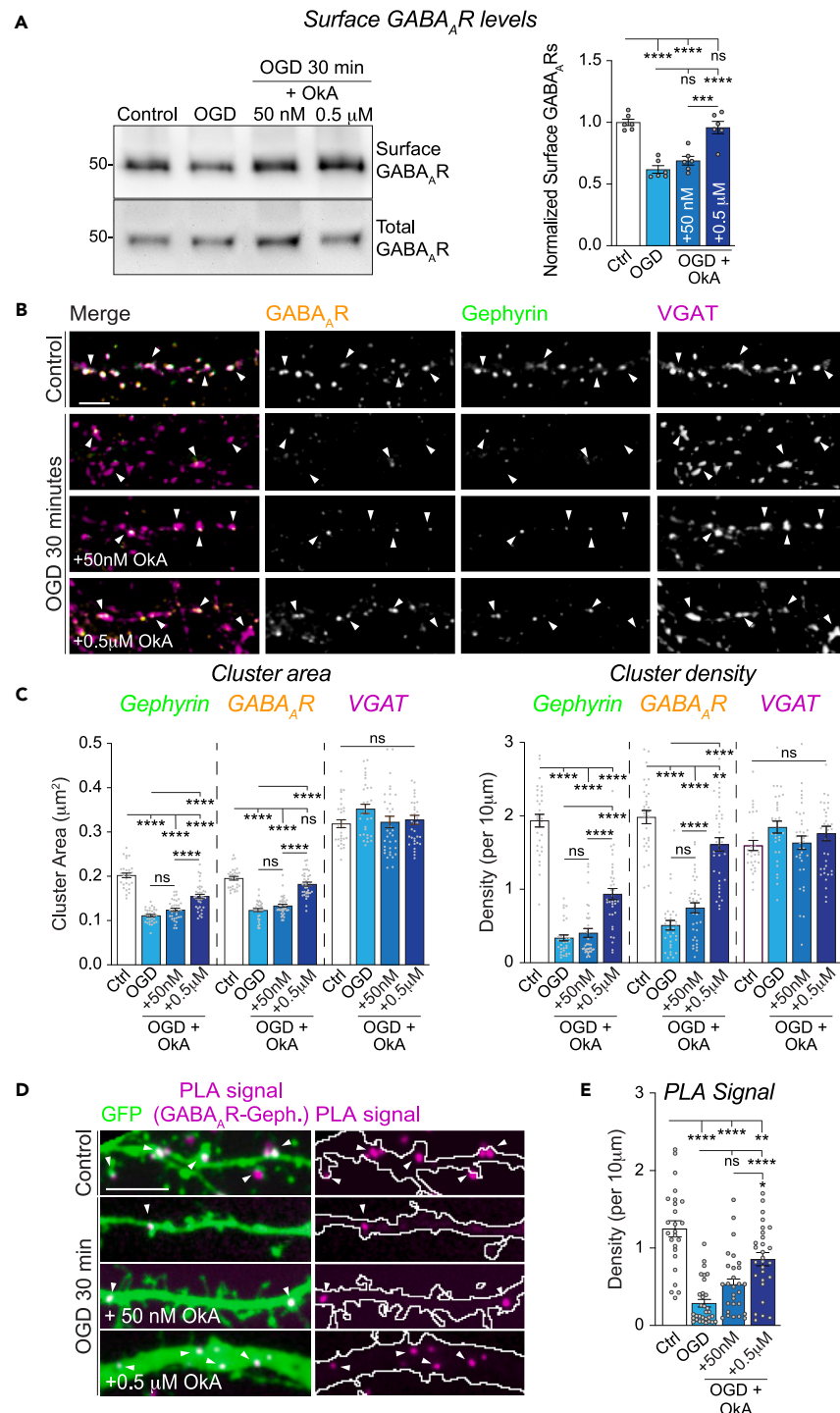
Figure 2. PP1α inhibition prevents OGD-induced GABA$_A$R surface removal but not their declustering from the synapse

(A) Surface biotinylation of hippocampal neurons treated to control or OGD conditions for 30 min in the presence of OkA at low (50 nM; selectively inhibits PP2A) or high (0.5 μM; inhibits PP2A and PP1α) concentrations. Quantification shows GABA$_A$R-α1 surface levels normalized to total levels (10% input), n = 6 independent experiments.

(B) Representative confocal images of dendritic segments from hippocampal neurons labeled for surface GABA$_A$R-γ2, gephyrin and VGAT. Neurons were treated with control or OGD conditions for 30 min in the presence of OkA (at 50 nM or 0.5 μM). Arrowheads indicate VGAT positive synapses. Scale bar = 5 μm.

(C) Quantification of synapse cluster area (left) and density (right) from images in (B), n = 30–36 neurons.

Figure 2. *Continued*

(D) Proximity ligation assay (PLA) for gephyrin and GABA$_A$R-α1 in GFP expressing hippocampal neurons. Representative dendritic segments show PLA signal (magenta) from neurons treated with control or OGD conditions for 30 min, in the presence of OkA (50 nM or 0.5 μM). Arrowheads indicate PLA-positive signal (representing the GABA$_A$R-gephyrin interaction). Scale = 5 μm.

(E) Quantification shows the density of the PLA signal, n = 25–32 neurons. Values represent mean ± SEM. *p ≤ 0.05, **p < 0.01, ***p < 0.001, ****p < 0.0001, one-way ANOVA, Bonferroni post hoc test (A, C, E).

GABA$_A$R-β3 subunit. The receptors are then targeted to lysosomes where they undergo degradation throughout early reperfusion, providing a key mechanism for the sustained loss of GABA$_A$R expression and synaptic inhibition observed during reperfusion injury. Together, these results place the trafficking and loss of synaptic GABA$_A$Rs within the context of rapid inhibitory synapse disassembly and elimination, and provide a more complete picture of the mechanisms driving the profound loss of inhibition which underscores excitotoxic neuronal hyper-excitability and delayed cell-death.

RESULTS

The temporal dynamics of GABA$_A$R internalization during OGD

OGD drives GABA$_A$R endocytosis and inhibitory synapse disassembly within 30 min of onset.[14,15] However, the precise time-point at which the receptors are internalized in the context of receptor declustering, gephyrin removal, and synapse disassembly is unknown (Figure 1A). To establish a timeline of GABA$_A$R removal from the plasma membrane during OGD, we first used surface biotinylation assays to monitor changes in levels of surface GABA$_A$Rs (containing α1 subunits) at increasing time-points during an *in vitro* OGD insult[14,15] (Figure 1B). GABA$_A$R surface levels remained stable at 5 min-post induction and only started to decrease at the 10 min timepoint, followed by an ∼65% reduction at 15 min (Figure 1B). To complement this experiment, we also performed antibody feeding assays to directly quantify the proportion of surface GABA$_A$Rs that are internalized during the OGD time-course (Figure 1C). Surface GABA$_A$Rs were live labeled with an N-terminal, extracellular antibody to the γ2 subunit enabling them to be tracked through the endosomal system to quantify 'internalized' and 'surface' receptor populations (Figure 1C). Line scans along each representative dendrite indicated an increase in the internalized pool of GABA$_A$Rs over time (magenta lines), which is in line with their removal from the plasma membrane (Figure 1D). Furthermore, analysis of surface and internalized receptor populations revealed significant increases in GABA$_A$R internalization index (internalized GABA$_A$Rs/(surface + internalized GABA$_A$Rs)) at 10 and 15 min post-OGD induction (Figures 1D and 1E), with minimal increase within the initial 5 min of OGD. Together, these experiments show that OGD leads to delayed internalization of GABA$_A$Rs starting at ∼10 min from OGD onset, presumably following the initial declustering of the receptors from the synaptic site.

PP1α inhibition prevents OGD-induced GABA$_A$R surface removal but not their declustering from the synapse

We previously showed that rapid OGD-mediated GABA$_A$R declustering is controlled by CaN, and gephyrin disassembly is driven by calpain, which act independently from each other.[14] The phosphatases PP2A and PP1α have both been shown to regulate GABA$_A$R endocytosis via the dephosphorylation of the GABA$_A$R-β3 subunit in a variety of contexts,[11,16,17] although a precise role for PP2A and/or PP1α in OGD-mediated GABA$_A$R endocytosis following receptor declustering has not been investigated. To first determine whether PP1α and/or PP2A are driving OGD-induced internalization, we exposed hippocampal neurons to OGD for 30 min in the presence of okadaic acid (OkA), which selectively inhibits PP2A at low concentrations (50 nM) and both PP2A and PP1α at higher concentrations (0.5 μM;[18]). We then performed surface biotinylation assays, to quantify surface GABA$_A$Rs levels, as in Figure 1B. As previously shown, OGD induced a robust decrease in surface GABA$_A$R levels after 30 min, compared to control conditions (Figure 2A; [14,15,19]). Surprisingly, this loss of surface GABA$_A$Rs was not impacted by the inclusion of 50 nM OkA during OGD, suggesting that PP2A does not have a significant role in GABA$_A$R surface loss. However, in comparison, OGD-induced surface removal of GABA$_A$Rs was fully prevented by the inclusion of 0.5 μM OkA (Figure 2A), indicating a role for PP1α in controlling OGD-mediated GABA$_A$R surface removal.

Having shown that PP1α activity was required for GABA$_A$R removal from the plasma membrane, we also asked whether its activity contributed to inhibitory synapse disassembly during OGD. We exposed cultured hippocampal neurons to a 30 min OGD insult, with low or high concentrations of OkA, and performed immunocytochemistry for surface GABA$_A$Rs, gephyrin and the inhibitory presynaptic marker, vesicular GABA transporter (VGAT,[14,20]; ; Figure 2B). Neuronal dendrites were imaged by confocal microscopy and analyzed to determine changes in both cluster area and density for each synaptic component (Figure 2C). As expected, following the OGD insult we observed a robust shrinkage in cluster area and density of GABA$_A$Rs and gephyrin, with no impact on the VGAT-positive presynaptic terminals (Figures 2B and 2C). Again, inhibition of PP2A alone had little effect on the loss of GABA$_A$Rs and gephyrin from the synapse, reflected by no significant difference between OGD and OGD +50 nM OkA conditions (Figures 2B and 2C). In contrast, blockade of PP1α activity with 0.5 μM OkA substantially, but not completely, prevented GABA$_A$R synaptic loss (Figures 2B and 2C). Gephyrin loss following OGD was also only partially restored by PP1α inhibition (Figures 2B and 2C), which is in agreement with calpain cleavage of gephyrin being the primary mechanism that drives gephyrin removal from synapses during OGD.[14]

PP1α-dependent restoration of GABA$_A$R synaptic clustering during OGD was incomplete, suggesting that PP1α may be primarily responsible for the loss of receptors from the neuronal cell surface, but not necessarily their declustering from GABAergic synaptic sites. To test this idea, we performed proximity ligation assays (PLAs) which we have previously used to measure the direct interaction between GABA$_A$Rs and gephyrin, and assessed the extent of the GABA$_A$R-gephyrin association following OGD and when PP2A or PP1α activity is inhibited. As

expected, the PLA signal (representing the GABA$_A$R-gephyrin interaction) was reduced by ~76% following 30 min of OGD, indicating reduced interaction between GABA$_A$Rs and gephyrin, presumably due to removal of both components from the synapse (Figures 2D and 2E). Our previous work showed that this effect was completely prevented by CaN inhibition by cyclosporin A (CsA), which is in agreement with the role of CaN in directly controlling receptor declustering immediately following OGD onset.[14] In comparison, blockade of PP1α activity only partially prevented the OGD-induced reduction in PLA signal (Figures 2D and 2E), indicating that some GABA$_A$R-gephyrin interactions are maintained during PP1α inhibition, likely through residual retention of gephyrin at the synapse, thereby contributing to the partial 'rescue' of synapses by PP1α inhibition. In contrast, we observed no recovery in GABA$_A$R-gephyrin interactions when PP2A alone is inhibited with 50 nM OkA. Together with our imaging data, these results indicate that PP1α is likely the main driver of receptor internalization during OGD, but its inhibition does not completely prevent synapse disassembly.

PP1α-dependent dephosphorylation of the GABA$_A$R-β3 subunit during GCI

During OGD, GABA$_A$R internalization is driven by interactions between a triple arginine motif '^{405}RRR^{407}' within the GABA$_A$R-β3 subunit intracellular domain (ICD) and the clathrin adaptor protein, AP2.[15,21] The GABA$_A$R-β2 subunit also interacts with AP2,[22] however GABA$_A$Rs containing the β3 subunit form a large proportion of GABA$_A$R subtypes in the hippocampus,[23,24] thus we focused our study on GABA$_A$R-β3. The GABA$_A$R-β3 subunit interaction with AP2 is controlled by the phosphorylation state of two proximal, downstream serine residues at 408/409 (β3-S408/409; Figure 3A), and are targets of dephosphorylation by PP1α and PP2A.[25,26] Reduced phosphorylation of this site promotes the GABA$_A$R-β3-AP2 interaction and receptor endocytosis, while increased phosphorylation prevents the interaction and inhibits receptor endocytosis.[21,22] To assess whether the GABA$_A$R-β3-S408/409 site is impacted during the early stages of OGD, we first assessed β3-S408/409 levels in lysates from hippocampal neurons exposed to OGD or control conditions for 30 min. Using a β3-S408/409 phospho-specific antibody, we found that β3-S408/409 phosphorylation levels were significantly reduced following 30 min OGD (Figure 3B). To verify whether this reduction in β3-S408/409 also occurred *in vivo* following GCI, we analyzed hippocampal tissue from mice that had undergone cardiac arrest and cardio-pulmonary resuscitation (CA/CPR) to induce GCI (see STAR Methods for details;[14,27]). We used this model, as CA/CPR produces direct ischemic injury and OGD to the hippocampus making it a good *in vivo* correlate for our *in vitro* OGD model.[28,29] Hippocampi were harvested immediately following the CA/CPR and recovery process (~40 min in total) to enable as close a comparison to our *in vitro* model as possible (Figure 3C; [14]). Probing hippocampal lysates for phospho-β3-S408/409 from CA/CPR or sham mice revealed a similar reduction in phosphorylation of this site as we observed *in vitro* (Figure 3C), indicating that this mechanism may also be important *in vivo*. To verify whether OGD-driven dephosphorylation of the β3-S408/409 site was mediated by PP2A or PP1α during OGD, we measured levels of phospho-β3-S408/409 in the presence of OkA at low and high concentrations. OGD-mediated reductions in phospho-β3-S408/409 levels were completely restored in the presence of 0.5 μM OkA, compared with very little recovery with lower OkA concentrations (Figure 3D). This result is consistent with a prominent role for PP1α in controlling OGD-driven GABA$_A$R surface removal, and hence dephosphorylation of this site. To determine the kinetics of β3-S408/409 dephosphorylation during OGD and whether this coincided with the timeline of GABA$_A$R internalization, we monitored β3-S408/409 levels throughout the OGD insult (Figure 3E). We found that the OGD-induced reduction in phospho-β3-S408/409 started between 9 and 12 min of OGD, with the maximal reduction in phosphorylation levels at 15 min of OGD (Figure 3E), which closely mirrored the time-course of receptor endocytosis (Figures 1B–1E). CaN and calpain activity are crucial for the initial, rapid synaptic declustering of GABA$_A$Rs and gephyrin, respectively.[14] Thus, we asked whether CaN and calpain might act directly upstream of GABA$_A$R-β3-S408/409 dephosphorylation. Inclusion of the CaN inhibitor CsA, or the calpain inhibitor, MDL-28170 (Calp-i), during the OGD insult revealed that neither calpain nor CaN inhibition could prevent the dephosphorylation of the β3-S408/409 site (Figures S1A–S1D), indicating that dephosphorylation of the receptor at β3-S408/409 during OGD is independent of these other calcium-mediated signaling pathways.

Having identified that OGD-induced GABA$_A$R internalization happens ~15 min into an OGD insult, and phospho-β3-S408/409 levels reduce within the same time frame, we then wanted to directly test whether PP1α was controlling GABA$_A$R internalization at this timepoint. To do this, we performed internalization assays during a 15 min OGD insult, with different concentrations of OkA. GABA$_A$Rs were readily internalized by the end of the 15 min OGD insult, and this was selectively inhibited with 0.5 μM OkA and not 50 nM OkA (Figures 3F and 3G), showing that PP1α controls OGD-driven GABA$_A$R internalization at this timepoint during OGD. Furthermore, inhibition of CaN also prevented receptor internalization, indicating that the CaN signaling that leads to OGD-induced GABA$_A$R declustering lies upstream of receptor internalization (Figures 3F and 3G). Thus, we conclude from these data that PP1α activity drives β3-S408/409 dephosphorylation and receptor internalization at ~15 min following OGD induction, and although GABA$_A$R internalization requires upstream CaN activity, the dephosphorylation of the GABA$_A$R itself is independent of CaN activity.

Reduced GABA$_A$R expression during post-ischemic reperfusion

We were then interested in the fate of GABA$_A$Rs following their internalization and the initial OGD insult during post-ischemia reperfusion. OGD-induced inhibitory synapse loss is sustained for at least 2 h of reperfusion following the initial OGD insult, suggesting that GABA$_A$R surface removal and synapse elimination is likely permanent.[14] However, the long-term fate of GABA$_A$Rs following the initial OGD insult is unknown. To investigate this, we assessed whether a reduction in GABA$_A$R protein levels following OGD and global ischemia could contribute to their permanent removal from the synapse. We first measured total GABA$_A$R subunit expression immediately following a 30 min OGD insult *in vitro*, and found that expression levels of γ2 and β3 subunits showed little change compared with controls (Figure 4A). This finding was recapitulated *in vivo*, indicating no change in GABA$_A$R expression levels immediately following CA/CPR when compared with sham controls
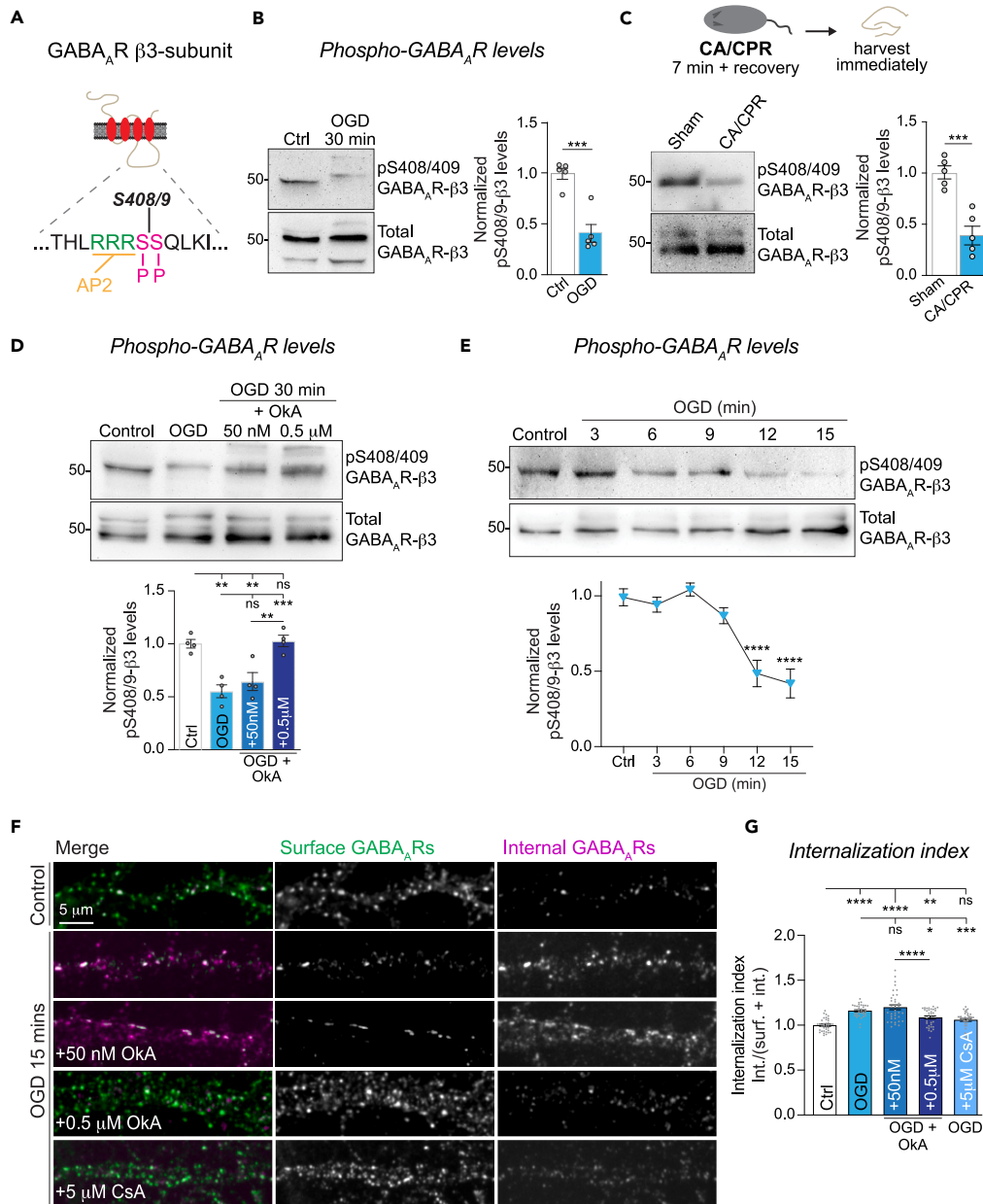
Figure 3. PP1α-dependent dephosphorylation of the GABA$_A$R-β3 subunit during global ischemia

(A) Cartoon of GABA$_A$R β3 subunit. The intracellular domain contains a triple arginine motif 'RRR' which mediates binding to AP2 and receptor endocytosis. Adjacent serine phospho-sites at 408/409 act as negative regulators of receptor endocytosis when phosphorylated.

(B–C) Hippocampal neuronal lysates analyzed following control or OGD insults for 30 min (*in vitro*; B) and hippocampal crude membrane lysates from mice post sham or CA/CPR procedure (*in vivo*; C). Phosphorylated β3-S408/409 levels were normalized to total GABA$_A$R-β3 levels, n = 5 independent cultures/animals.

(D) Hippocampal neuronal lysates analyzed following a 30 min OGD insult in the presence of OkA (50 nM or 0.05 μM). Phosphorylated β3-S408/409 levels were normalized to total GABA$_A$R-β3 levels, n = 4 independent experiments.

(E) Hippocampal lysates analyzed following OGD at 3 min intervals up to a maximum of a 15 min. Phosphorylated β3-S408/409 levels were normalized to total GABA$_A$R-β3 levels, n = 5 independent experiments.

(F) Representative confocal images of dendritic segments from hippocampal neurons live-labeled for surface GABA$_A$R-γ2 and treated to control or OGD conditions for 30 min in the presence OkA at either concentration (50 nM or 0.05 μM), or CsA. Scale bar = 5 μm.

(G) Quantification of the internalization index, n = 35–36 neurons. Values represent mean ± SEM. Data in (B), (D), (E) & (F) were normalized to control conditions. *p ≤ 0.05, **p < 0.01, ***p < 0.001, ****p < 0.0001, Student's *t* test (B, C) or one-way ANOVA, Bonferroni post hoc test (D, E, G). See also Figure S1.
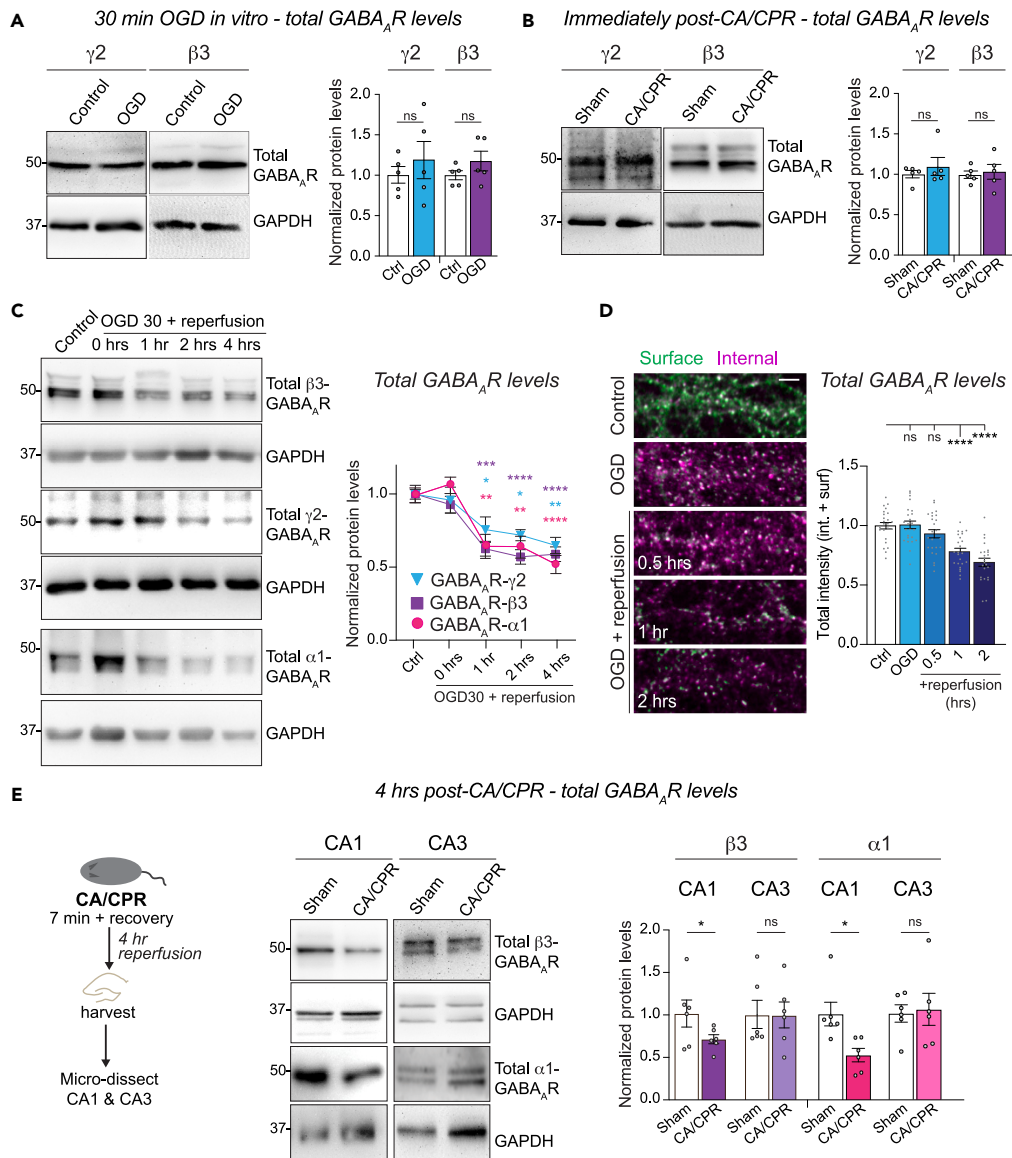
Figure 4. Reduced GABA$_A$R expression during post-OGD reperfusion

(A) Hippocampal neuronal lysates harvested following 30 min control or OGD treatment. GABA$_A$R-γ2 or β3 levels were normalized to GAPDH levels, n = 5 independent experiments.

(B) Hippocampal crude membrane lysates from mice immediately following sham or CA/CPR surgeries. GABA$_A$R-γ2 or β3 levels were normalized to GAPDH levels, n = 5 independent experiments.

(C) Hippocampal neuronal lysates analyzed following reperfusion up to 4 h after a 30 min OGD insult. Total GABA$_A$R-γ2, -β3 and -α1 levels were normalized to GAPDH levels, n = 5–6 independent experiments. Colored stars compare statistical significance to control condition for each subunit.

(D) Representative confocal images of dendritic segments from hippocampal neurons live-labeled for surface GABA$_A$R-γ2 and treated to control or OGD conditions at different time-points following reperfusion injury. Scale = 5μm. Quantification of total GABA$_A$R intensity (internal + surface), n = 33–36 neurons.

(E) Hippocampal crude membrane lysates were isolated from CA1 and CA3 subregions following 4 h of reperfusion after sham or CA/CPR surgeries. GABA$_A$R-β3 and -α1 levels were normalized to GAPDH levels, n = 6 independent experiments. Values represent mean ± SEM. *p ≤ 0.05, **p < 0.01, ***p < 0.001, ****p < 0.0001, Student's t test (A, B, E), one-way ANOVA, Bonferroni post hoc test (C, D). See also Figures S2 and S3.

(Figure 4B). However, measurement of GABA$_A$R levels following increasing time-points of reperfusion revealed reduced β3, γ2 and α1 expression levels by ∼30% after 1 h reperfusion, followed by a continual reduction in expression up to 4 h post-insult (Figure 4C). This was in contrast to the expression of GluA1-AMPARs, which remained stable throughout OGD and the subsequent reperfusion phase, indicating this was not a blanket effect on all neurotransmitter receptors (Figure S2). To verify that GABA$_A$Rs specifically expressed at the neuronal surface are being downregulated throughout the reperfusion process, we performed internalization assays during the 30 min OGD insult and measured surface

and internalized receptor populations throughout reperfusion. As expected, GABA$_A$R internalization was elevated following the OGD insult and remained elevated throughout the duration of reperfusion (Figure S3A). In comparison, we calculated the total mean fluorescence intensity of receptors (surface + internal populations) at 30 min of OGD and found it was the same as controls, indicating that total protein levels remained intact. However, the total intensity of all the GABA$_A$Rs reduced with increasing lengths of reperfusion (Figure 4D), which is in agreement with our western blotting data that indicate reductions in total receptor expression during reperfusion likely follows their initial internalization during the OGD insult. Lastly, we assessed whether GABA$_A$R expression was also reduced following reperfusion *in vivo*, by measuring GABA$_A$R protein levels in hippocampal tissue ~4 h following CA/CPR (Figure 4E). Given that the CA3 hippocampal region is more resistant to ischemic insult than CA1, we micro-dissected each region and measured total GABA$_A$R levels (Figure 4E). Corroborating our *in vitro* data, GABA$_A$R β3 and α1 subunit levels were significantly reduced in tissue from the CA1 subregion following reperfusion injury, compared with tissue from sham mice (Figure 4E). In contrast, GABA$_A$R levels remained similar to sham controls in the CA3 subregion (Figure 4E), suggesting that differential mechanisms underlie persistent synaptic loss in these two hippocampal subregions. Together, these results indicate that expression of the major synaptic GABA$_A$R subtypes is reduced during ischemic reperfusion injury, and this may be a specific mechanism within the highly vulnerable CA1 region of hippocampus.

Internalized GABA$_A$Rs are targeted to the lysosome for degradation during ischemic reperfusion injury

Following their internalization, GABA$_A$Rs are trafficked through the endosomal network and either targeted for recycling back to the neuronal surface or to the lysosome for degradation.[30–32] Given the profound loss of internalized receptors throughout the reperfusion phase following OGD, we speculated that GABA$_A$Rs were likely being targeted for lysosomal degradation. To test this hypothesis, we tracked internalized GABA$_A$Rs using internalization assays and assessed their localization with the lysosomal marker, LAMP1, directly following OGD or during reperfusion (Figure 5A). We found a significant increase in GABA$_A$R-LAMP1 colocalization by the end of the 30 min OGD insult, and the localization of GABA$_A$Rs to LAMP1-positive lysosomes remained elevated throughout the reperfusion phase (Figure 5A). This result suggests that GABA$_A$Rs are targeted to the lysosome during the initial OGD insult, likely following their internalization at the 15 min timepoint. To test this hypothesis directly, we inhibited lysosomal degradation with the lysosomal inhibitor, leupeptin, for 2 h prior to, and throughout the OGD insult and reperfusion phases ([33]; Figures 5B–5D). Lysosomal blockade completely restored the elevated GABA$_A$R-LAMP1 colocalization we observed following OGD and reperfusion down to control levels (2 h; Figure 5B). Furthermore, reduced GABA$_A$R expression levels following reperfusion (measured by both western blotting and immunofluorescence) was completely alleviated with leupeptin application, confirming that GABA$_A$Rs are degraded by the lysosome during reperfusion injury (Figures 5C and 5D). As reductions in GABA$_A$R mRNA levels could also contribute sustained reductions in total protein levels following OGD, we also analyzed GABA$_A$R mRNA levels during reperfusion injury using RT-qPCR, and found that GABA$_A$R γ2 and β3 mRNA levels were indeed reduced by ~25% following the 30 min OGD insult (Figure S3). This reduction was maintained for several hours of reperfusion, suggesting that reduced transcription and/or translation may also contribute to sustained reductions in GABA$_A$R levels during OGD reperfusion injury. Taken together, our data suggest that trafficking of GABA$_A$Rs to lysosomal compartments for increased receptor degradation is a key mechanism for sustained receptor loss from synaptic sites, with likely contributions from impaired GABA$_A$R production.

DISCUSSION

Impaired synaptic inhibition is a hallmark of excitotoxic brain injury, leading to hyper-activity of neuronal networks, and contributing to delayed cell-death of highly vulnerable neuronal populations.[4,10] In this study we investigated the timeline of GABA$_A$R trafficking throughout an ischemic insult and the subsequent reperfusion phase, and placed this process in the context of the rapid, stepwise inhibitory synapse disassembly which is initiated within the first few minutes of the insult.[14] We find that GABA$_A$R internalization happens ~15 min from OGD onset and is regulated by PP1α activity and the GABA$_A$R-β3-S408/409 phosphorylation site. Our results show that following internalization, GABA$_A$Rs are targeted to lysosomes (as early as 30 min post-OGD induction) and degraded, leading to a progressive reduction in total GABA$_A$R expression throughout cumulative hours of reperfusion, both *in vitro* and *in vivo*. This work both provides temporal details of the trafficking itinerary of GABA$_A$Rs once they have dispersed from the synapse (~5 min post-OGD induction), but also points to the mechanisms that underlie them. In addition, our results show that GABA$_A$Rs are not just transiently lost from synapses, but are permanently degraded, accounting for the long-term loss of GABAergic synapses following ischemia and the persistent reduction of inhibition following reperfusion.[4,12,14,34]

Our recent work showed that GABAergic synapses are disassembled and eliminated quickly following the onset of ischemia, presumably initiating the profound loss of synaptic inhibition that is reported hours to days following the initial ischemic insult.[4,12,14] GABA$_A$R synaptic declustering and gephyrin cleavage happens within the first 10 min of OGD onset, leading to elimination of ~50% of synapses by 30 min OGD.[14] GABA$_A$Rs have long been known to undergo OGD-induced endocytosis within this 30 min time frame, but there is little detail of when precisely this happens.[15,19] Here we find that GABA$_A$Rs are in fact internalized early on during OGD, beginning at the 10 min timepoint, with substantial internalization by 15 min. This timeline fits well in the broader context of synapse elimination, as it directly follows initial receptor declustering (~5 min), which would increase the availability of surface mobile receptors that could be captured by endocytic zones for internalization.[15] Notably, as the gephyrin scaffold is also being concurrently disassembled at ~10 min post-OGD induction, the likelihood of receptors being restabilized at the synapse is low, thereby promoting receptor mobility on the cell surface, and ultimately receptor internalization.
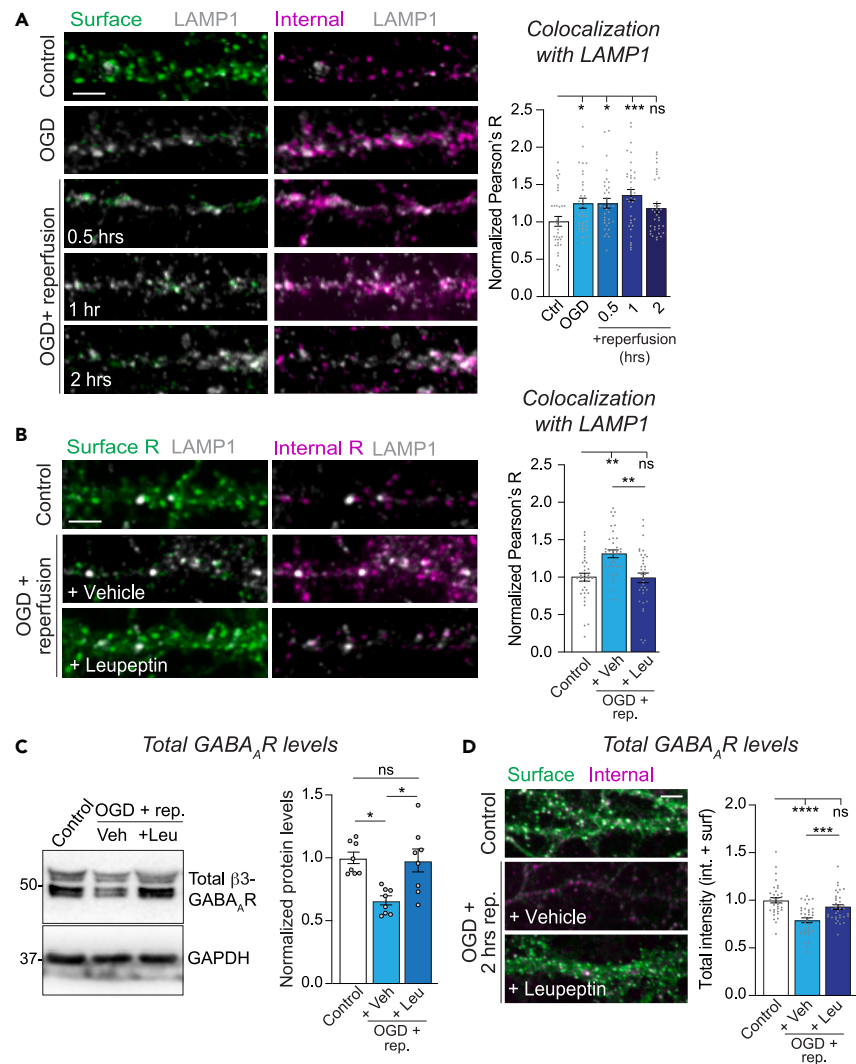
Figure 5. Internalized GABA$_A$Rs are targeted to the lysosome for degradation during ischemic reperfusion injury

(A) Representative confocal images of dendritic segments from hippocampal neurons live-labeled for surface GABA$_A$R-γ2 and treated to control or OGD conditions at different time-points following reperfusion injury. Neurons were labeled with antibodies to lysosomal marker LAMP1 and colocalization between internalized GABA$_A$Rs and LAMP1 was calculated by Pearson's coefficient. Quantification shows normalized Pearson's coefficient, n = 36 neurons per condition. Scale = 5 μm.

(B) Representative confocal images of dendritic segments from hippocampal neurons live-labeled for surface GABA$_A$R-γ2 and underwent OGD + reperfusion (2 h), with or without leupeptin. Neurons were labeled with antibodies to lysosomal marker LAMP1 and colocalization between internalized GABA$_A$Rs and LAMP1 was calculated by Pearson's coefficient. Quantification shows normalized Pearson's coefficient, n = 36 neurons per condition. Scale = 5 μm.

(C) Hippocampal neuronal lysates harvested following a 30 min control or OGD insult + reperfusion (2 h) in the presence of leupeptin. GABA$_A$R-β3 levels were normalized to GAPDH levels, n = 8 independent experiments.

(D) Representative confocal images of dendritic segments from hippocampal neurons live-labeled for surface GABA$_A$R-γ2 and treated to control or OGD conditions + reperfusion in the presence of leupeptin. Scale = 5μm. Quantification of total GABA$_A$R fluorescence (surface + internalized), n = 36 neurons. Scale = 5 μm. Values represent mean $\pm$ SEM. *p $\leq$ 0.05, **p < 0.01, ***p < 0.001, ****p < 0.0001, one-way ANOVA, Bonferroni post hoc test.

GABAergic synapse disassembly following the onset of ischemia is controlled by CaN, which drives receptor dispersal from the synapse, and calpain, which cleaves gephyrin, therefore shrinking and removing the gephyrin scaffold.[14,35] We found that PP1α activity is required for GABA$_A$R internalization at 15 min following OGD induction, and likely dephosphorylates the β3-S408/409 site at this timepoint to enable binding to AP2 and recruitment to endocytic zones. CaN and calpain are likely activated by increasing concentrations of Ca^{2+} as the ischemic insult progresses, whereby CaN is activated rapidly by low Ca^{2+} levels and calpain is activated several minutes later by higher concentrations. On the other hand, PP1α can be activated over slower timescales by a variety of stimuli, including TNFα[16] and by altered interactions with the inhibitory scaffold, PRIP-1.[26] In these situations, PKA-mediated phosphorylation of PRIP-1 following increased GPCR activity derepresses

PP1α, allowing it to act on downstream targets such as GABA_AR-β3-S408/409.[26] Thus, β3-S408/9 dephosphorylation is probably not directly influenced directly by Ca^{2+}, but through upstream signaling cascades that require more time to act on downstream targets, which fits well with the likely delayed activation of PP1α compared to CaN during the OGD process. The β3-S408/9 phospho-site is also a target of PP2A-mediated dephosphorylation in multiple circumstances.[17,36] However, we found that inhibition of PP2A with low concentrations of OkA had no effect on OGD-induced GABA_AR internalization or synapse disassembly, so we conclude the primary regulator of GABA_AR trafficking at these early stages of OGD is likely PP1α.

Our imaging experiments show that OGD-induced GABA_AR synaptic declustering and the GABA_AR-gephyrin interaction is only partially recovered when PP1α is inhibited. One explanation for this is that although endocytosis of GABA_ARs is blocked, they are still likely dispersed from synapses due to upstream CaN activation. This could lead to increased 'free' surface receptors that are not captured by endocytic zones, and these receptors could be stabilized back at the synapse by remaining gephyrin. Gephyrin clustering is also partially restored by inhibiting PP1α-mediated endocytosis during OGD and this is also observed, to a greater extent, upon CaN inhibition to prevent OGD-induced receptor declustering.[14] This effect likely reflects the co-dependency of GABA_ARs and gephyrin on each other for their stability and the ability of the gephyrin scaffold to be clustered by the receptors themselves, so that when GABA_ARs are reclustered at the synaptic site, some gephyrin is also able to remain.[37–39] Furthermore, this underscores the likely importance of other scaffolds and receptor stabilizing molecules, that in addition to gephyrin, contribute to receptor clustering and synapse stability.[40–42]

We have previously shown that inhibitory synapse loss persists following an ischemic insult, suggesting that GABA_AR removal from the plasma membrane is likely permanent.[14] However, the mechanisms that underlie this process are unclear. Our data show that GABA_AR levels decrease to ∼50% of control during reperfusion phase, both *in vitro* and *in vivo*, suggesting that reduced expression of GABA_ARs leads to the prolonged synaptic loss observed. We evaluated GABA_AR sorting through the endosomal pathway and observed co-localization of internalized GABA_ARs with the lysosomal marker LAMP1 at 30 min post-OGD and throughout the reperfusion phase. This was coupled with increased degradation of GABA_ARs (reflected by reduced total protein levels and surfaced labeled receptors) beginning around 1 h post-reperfusion. Inhibiting the lysosome with leupeptin blocked GABA_AR loss during reperfusion, suggesting that lysosomal-dependent degradation is the main route for decreasing receptor expression following excitotoxicity. Intriguingly, *in vivo*, reduced GABA_AR protein expression was specific to the CA1 region of hippocampus, with no reduction in CA3, suggesting potentially region-specific mechanisms that alter GABAergic synaptic function during GCI. This is also in agreement with our recent finding that GABAergic synapses are drastically downregulated in *stratum radiatum* and *stratum pyramidale* of CA1 following CA/CPR.[14] Put together, these observations are consistent with CA1 being highly vulnerable to ischemic insult and exhibiting a high level of delayed cell-death,[43,44] whereas CA3 is more resilient to cell-death during excitotoxic injury.[13,45] Future studies exploring the impact of GCI on GABA_AR trafficking and clustering within other hippocampal subregions, and across other brain regions will be crucial to assess how generalized the mechanisms described here may be.

A possible mechanism driving OGD-induced lysosomal targeting could be ubiquitination of the GABA_AR itself, a process that is important for regulation of normal GABA_AR trafficking and inhibitory synaptic function.[32,46,47] GABA_AR-γ2 subunits are readily ubiquitinated, which targets the receptor for degradation,[32] and this process is likely controlled by the ubiquitin E3 ligase RNF34.[47] An alternative or additional mechanism could involve the Arf-GEF protein, BIG3, which likely contributes to GABA_AR degradation through its localization to lysosomes.[48] GABA_AR receptor recycling is reduced during OGD, which also contributes to GABA_AR targeting for lysosomal degradation.[49] GABA_ARs are recycled under basal conditions, a process that is directed by key interaction protein, HAP1.[30,31] HAP1 is degraded during OGD, leading to reduced receptor recycling and enhanced receptor degradation.[49] Therefore, we speculate that a combination of increased GABA_AR ubiquitination, reduced HAP1 expression and contributions from other trafficking molecules likely underlie the progressive degradation of GABA_ARs during ischemic reperfusion injury. Furthermore, we also observed a potential reduction in GABA_AR production, reflected by a reduced number of GABA_AR transcripts, both throughout OGD and in the reperfusion phase, suggesting that transcription may be turned off early on throughout the process. This is in agreement with previous observations of reduced GABA_AR mRNA levels in hippocampal regions hours to days following an ischemic insult,[34] and is likely a complimentary mechanism to reduce expression levels of GABA_ARs long-term.

LIMITATIONS OF THE STUDY

We have shown that several aspects of the GABA_AR trafficking mechanisms described during OGD *in vitro* are likely conserved *in vivo*. However, we have not shown that the trafficking dynamics are the same *in vivo*, and we cannot differentiate between cell types in the hippocampal lysates from the *in vivo* model. Further imaging in hippocampal slices from the CA/CPR model will enable investigation of this more fully.

STAR★METHODS

Detailed methods are provided in the online version of this paper and include the following:

- KEY RESOURCES TABLE
- RESOURCE AVAILABILITY
  - ○ Lead contact
  - ○ Materials availability
  - ○ Data and code availability

- EXPERIMENTAL MODEL AND STUDY PARTICIPANT DETAILS
  - Dissociated hippocampal cultures
  - Cardiac arrest and cardiopulmonary resuscitation animal model
- METHOD DETAILS
  - Oxygen glucose deprivation (OGD) treatments *in vitro*
  - Immunocytochemistry (ICC)
  - Proximity Ligation Assay (PLA)
  - Antibody feeding assay
  - Image acquisition and analysis
  - Surface biotinylation
  - Western blotting
  - RNA isolation and RT-qPCR
- QUANTIFICATION AND STATISTICAL ANALYSIS

SUPPLEMENTAL INFORMATION

Supplemental information can be found online at https://doi.org/10.1016/j.isci.2023.108061.

AUTHOR CONTRIBUTIONS

Conceptualization, K.R.S. and J.D.G.; Formal Analysis and Investigation, J.D.G., S.E.G., E.T., A.R.S., S.E.W., and M.B.G.; Writing – Original Draft, J.D.G.; Writing – Review and Editing, J.D.G. and K.R.S.; Supervision, K.R.S. and N.Q.; Funding Acquisition, K.R.S., J.D.G., and N.Q.

DECLARATION OF INTERESTS

The authors declare no competing interests.

REFERENCES

1. Klausberger, T., and Somogyi, P. (2008). Neuronal diversity and temporal dynamics: the unity of hippocampal circuit operations. Science *321*, 53–57. https://doi.org/10.1126/science.1149381.

2. Chiu, C.Q., Barberis, A., and Higley, M.J. (2019). Preserving the balance: diverse forms of long-term GABAergic synaptic plasticity. Nat. Rev. Neurosci. *20*, 272–281. https://doi.org/10.1038/s41583-019-0141-5.

3. Fritschy, J.M. (2008). Epilepsy, E/I Balance and GABA(A) Receptor Plasticity. Front. Mol. Neurosci. *1*, 5. https://doi.org/10.3389/neuro.02.005.2008.

4. Mele, M., Costa, R.O., and Duarte, C.B. (2019). Alterations in GABA(A)-Receptor Trafficking and Synaptic Dysfunction in Brain Disorders. Front. Cell. Neurosci. *13*, 77. https://doi.org/10.3389/fncel.2019.00077.

5. Gao, R., and Penzes, P. (2015). Common mechanisms of excitatory and inhibitory imbalance in schizophrenia and autism spectrum disorders. Curr. Mol. Med. *15*, 146–167.

6. Lorenz-Guertin, J.M., and Jacob, T.C. (2018). GABA type a receptor trafficking and the architecture of synaptic inhibition. Dev. Neurobiol. *78*, 238–270. https://doi.org/10.1002/dneu.22536.

7. Tyagarajan, S.K., and Fritschy, J.M. (2014). Gephyrin: a master regulator of neuronal function? Nat. Rev. Neurosci. *15*, 141–156. https://doi.org/10.1038/nrn3670.

8. Nusser, Z., Hájos, N., Somogyi, P., and Mody, I. (1998). Increased number of synaptic GABA(A) receptors underlies potentiation at hippocampal inhibitory synapses. Nature *395*, 172–177.

9. Barberis, A. (2020). Postsynaptic plasticity of GABAergic synapses. Neuropharmacology *169*, 107643. https://doi.org/10.1016/j.neuropharm.2019.05.020.

10. El-Hassar, L., Esclapez, M., and Bernard, C. (2007). Hyperexcitability of the CA1 hippocampal region during epileptogenesis. Epilepsia *48* (*Suppl 5*), 131–139. https://doi.org/10.1111/j.1528-1167.2007.01301.x.

11. Mele, M., Ribeiro, L., Inácio, A.R., Wieloch, T., and Duarte, C.B. (2014). GABA(A) receptor dephosphorylation followed by internalization is coupled to neuronal death in *in vitro* ischemia. Neurobiol. Dis. *65*, 220–232. https://doi.org/10.1016/j.nbd.2014.01.019.

12. Zhan, R.-Z., Nadler, J.V., and Schwartz-Bloom, R.D. (2006). Depressed responses to applied and synaptically-released GABA in CA1 pyramidal cells, but not in CA1 interneurons, after transient forebrain ischemia. J. Cereb. Blood Flow Metab. *26*, 112–124.

13. Epsztein, J., Milh, M., Bihi, R.I., Jorquera, I., Ben-Ari, Y., Represa, A., and Crépel, V. (2006). Ongoing Epileptiform Activity in the Post-Ischemic Hippocampus Is Associated with a Permanent Shift of the Excitatory–Inhibitory Synaptic Balance in CA3 Pyramidal Neurons. J. Neurosci. *26*, 7082–7092. https://doi.org/10.1523/jneurosci.1666-06.2006.

14. Garcia, J.D., Gookin, S.E., Crosby, K.C., Schwartz, S.L., Tiemeier, E., Kennedy, M.J., Dell'Acqua, M.L., Herson, P.S., Quillinan, N., and Smith, K.R. (2021). Stepwise disassembly of GABAergic synapses during pathogenic excitotoxicity. Cell Rep. *37*, 110142. https://doi.org/10.1016/j.celrep.2021.110142.

15. Smith, K.R., Muir, J., Rao, Y., Browarski, M., Gruenig, M.C., Sheehan, D.F., Haucke, V.,

and Kittler, J.T. (2012). Stabilization of GABA(A) receptors at endocytic zones is mediated by an AP2 binding motif within the GABA(A) receptor beta3 subunit. J. Neurosci. *32*, 2485–2498. https://doi.org/10.1523/JNEUROSCI.1622-11.2011.

16. Pribiag, H., and Stellwagen, D. (2013). TNF-alpha downregulates inhibitory neurotransmission through protein phosphatase 1-dependent trafficking of GABA(A) receptors. J. Neurosci. *33*, 15879–15893. https://doi.org/10.1523/JNEUROSCI.0530-13.2013.

17. Terunuma, M., Xu, J., Vithlani, M., Sieghart, W., Kittler, J., Pangalos, M., Haydon, P.G., Coulter, D.A., and Moss, S.J. (2008). Deficits in phosphorylation of GABA(A) receptors by intimately associated protein kinase C activity underlie compromised synaptic inhibition during status epilepticus. J. Neurosci. *28*, 376–384. https://doi.org/10.1523/JNEUROSCI.4346-07.2008.

18. Favre, B., Turowski, P., and Hemmings, B.A. (1997). Differential inhibition and posttranslational modification of protein phosphatase 1 and 2A in MCF7 cells treated with calyculin-A, okadaic acid, and tautomycin. J. Biol. Chem. *272*, 13856–13863. https://doi.org/10.1074/jbc.272.21.13856.

19. Mielke, J.G., and Wang, Y.T. (2005). Insulin exerts neuroprotection by counteracting the decrease in cell-surface GABA receptors following oxygen-glucose deprivation in cultured cortical neurons. J. Neurochem. *92*, 103–113.

20. Rajgor, D., Purkey, A.M., Sanderson, J.L., Welle, T.M., Garcia, J.D., Dell'Acqua, M.L., and Smith, K.R. (2020). Local miRNA-Dependent Translational Control of GABA(A)R Synthesis during Inhibitory Long-Term Potentiation. Cell Rep. *31*, 107785. https://doi.org/10.1016/j.celrep.2020.107785.

21. Smith, K.R., McAinsh, K., Chen, G., Arancibia-Carcamo, I.L., Haucke, V., Yan, Z., Moss, S.J., and Kittler, J.T. (2008). Regulation of inhibitory synaptic transmission by a conserved atypical interaction of GABA(A) receptor beta- and gamma-subunits with the clathrin AP2 adaptor. Neuropharmacology *55*, 844–850. S0028-3908(08)00242-6 [pii]. https://doi.org/10.1016/j.neuropharm.2008.06.072.

22. Kittler, J.T., Chen, G., Honing, S., Bogdanov, Y., McAinsh, K., Arancibia-Carcamo, I.L., Jovanovic, J.N., Pangalos, M.N., Haucke, V., Yan, Z., and Moss, S.J. (2005). Phospho-dependent binding of the clathrin AP2 adaptor complex to GABAA receptors regulates the efficacy of inhibitory synaptic transmission. Proc. Natl. Acad. Sci. USA *102*, 14871–14876. https://doi.org/10.1073/pnas.0506653102.

23. Laurie, D.J., Wisden, W., and Seeburg, P.H. (1992). The distribution of thirteen GABAA receptor subunit mRNAs in the rat brain. III. Embryonic and postnatal development. J. Neurosci. *12*, 4151–4172. https://doi.org/10.1523/JNEUROSCI.12-11-04151.1992.

24. Wisden, W., Laurie, D.J., Monyer, H., and Seeburg, P.H. (1992). The distribution of 13 GABAA receptor subunit mRNAs in the rat brain. I. Telencephalon, diencephalon, mesencephalon. J. Neurosci. *12*, 1040–1062. https://doi.org/10.1523/JNEUROSCI.12-03-01040.1992.

25. Kanematsu, T., Fujii, M., Mizokami, A., Kittler, J.T., Nabekura, J., Moss, S.J., and Hirata, M. (2007). Phospholipase C-related inactive protein is implicated in the constitutive internalization of GABAA receptors mediated by clathrin and AP2 adaptor complex. J. Neurochem. *101*, 898–905.

26. Terunuma, M., Jang, I.S., Ha, S.H., Kittler, J.T., Kanematsu, T., Jovanovic, J.N., Nakayama, K.I., Akaike, N., Ryu, S.H., Moss, S.J., and Hirata, M. (2004). GABAA receptor phospho-dependent modulation is regulated by phospholipase C-related inactive protein type 1, a novel protein phosphatase 1 anchoring protein. J. Neurosci. *24*, 7074–7084. https://doi.org/10.1523/JNEUROSCI.1323-04.2004.

27. Buonarati, O.R., Cook, S.G., Goodell, D.J., Chalmers, N.E., Rumian, N.L., Tullis, J.E., Restrepo, S., Coultrap, S.J., Quillinan, N., Herson, P.S., and Bayer, K.U. (2020). CaMKII versus DAPK1 Binding to GluN2B in Ischemic Neuronal Cell Death after Resuscitation from Cardiac Arrest. Cell Rep. *30*, 1–8.e4. https://doi.org/10.1016/j.celrep.2019.11.076.

28. Papadimitriou, D., Xanthos, T., Dontas, I., Lelovas, P., and Perrea, D. (2008). The use of mice and rats as animal models for cardiopulmonary resuscitation research. Lab. Anim. *42*, 265–276. https://doi.org/10.1258/la.2007.006035.

29. Traystman, R.J. (2003). Animal models of focal and global cerebral ischemia. ILAR J. *44*, 85–95. https://doi.org/10.1093/ilar.44.2.85.

30. Kittler, J.T., Thomas, P., Tretter, V., Bogdanov, Y.D., Haucke, V., Smart, T.G., and Moss, S.J. (2004). Huntingtin-associated protein 1 regulates inhibitory synaptic transmission by modulating gamma-aminobutyric acid type A receptor membrane trafficking. Proc. Natl. Acad. Sci. USA *101*, 12736–12741.

31. Twelvetrees, A.E., Yuen, E.Y., Arancibia-Carcamo, I.L., MacAskill, A.F., Rostaing, P., Lumb, M.J., Humbert, S., Triller, A., Saudou, F., Yan, Z., and Kittler, J.T. (2010). Delivery of GABAARs to synapses is mediated by HAP1-KIF5 and disrupted by mutant huntingtin. Neuron *65*, 53–65. https://doi.org/10.1016/j.neuron.2009.12.007.

32. Arancibia-Cárcamo, I.L., Yuen, E.Y., Muir, J., Lumb, M.J., Michels, G., Saliba, R.S., Smart, T.G., Yan, Z., Kittler, J.T., and Moss, S.J. (2009). Ubiquitin-dependent lysosomal targeting of GABA(A) receptors regulates neuronal inhibition. Proc. Natl. Acad. Sci. USA *106*, 17552–17557.

33. Fernández-Monreal, M., Brown, T.C., Royo, M., and Esteban, J.A. (2012). The balance between receptor recycling and trafficking toward lysosomes determines synaptic strength during long-term depression. J. Neurosci. *32*, 13200–13205. https://doi.org/10.1523/JNEUROSCI.0061-12.2012.

34. Li, H., Siegel, R., and Schwartz, R. (1993). Rapid decline of GABAA receptor subunit mRNA expression in hippocampus following transient cerebral ischemia in the gerbil. Hippocampus *3*, 527–537.

35. Costa, J.T., Mele, M., Baptista, M.S., Gomes, J.R., Ruscher, K., Nobre, R.J., de Almeida, L.P., Wieloch, T., and Duarte, C.B. (2016). Gephyrin Cleavage in In Vitro Brain Ischemia Decreases GABAA Receptor Clustering and Contributes to Neuronal Death. Mol. Neurobiol. *53*, 3513–3527. https://doi.org/10.1007/s12035-015-9283-2.

36. Jovanovic, J.N., Thomas, P., Kittler, J.T., Smart, T.G., and Moss, S.J. (2004). Brain-derived neurotrophic factor modulates fast synaptic inhibition by regulating GABA(A) receptor phosphorylation, activity, and cell-surface stability. J. Neurosci. *24*, 522–530.

37. Essrich, C., Lorez, M., Benson, J.A., Fritschy, J.-M., and Lüscher, B. (1998). Postsynaptic clustering of major GABAA receptor subtypes requires the gamma 2 subunit and gephyrin. Nat. Neurosci. *1*, 563–571.

38. Panzanelli, P., Gunn, B.G., Schlatter, M.C., Benke, D., Tyagarajan, S.K., Scheiffele, P., Belelli, D., Lambert, J.J., Rudolph, U., and Fritschy, J.M. (2011). Distinct mechanisms regulate GABAA receptor and gephyrin clustering at perisomatic and axo-axonic synapses on CA1 pyramidal cells. J. Physiol. *589*, 4959–4980. https://doi.org/10.1113/jphysiol.2011.216028.

39. Schweizer, C., Balsiger, S., Bluethmann, H., Mansuy, I.M., Fritschy, J.M., Mohler, H., and Lüscher, B. (2003). The gamma 2 subunit of GABA(A) receptors is required for maintenance of receptors at mature synapses. Mol. Cell. Neurosci. *24*, 442–450. https://doi.org/10.1016/s1044-7431(03)00202-1.

40. Smith, K.R., Davenport, E.C., Wei, J., Li, X., Pathania, M., Vaccaro, V., Yan, Z., and Kittler, J.T. (2014). GIT1 and betaPIX are essential for GABA(A) receptor synaptic stability and inhibitory neurotransmission. Cell Rep. *9*, 298–310. https://doi.org/10.1016/j.celrep.2014.08.061.

41. Davenport, E.C., Pendolino, V., Kontou, G., McGee, T.P., Sheehan, D.F., López-Doménech, G., Farrant, M., and Kittler, J.T. (2017). An Essential Role for the Tetraspanin LHFPL4 in the Cell-Type-Specific Targeting and Clustering of Synaptic GABAA Receptors. Cell Rep. *21*, 70–83. https://doi.org/10.1016/j.celrep.2017.09.025.

42. Yamasaki, T., Hoyos-Ramirez, E., Martenson, J.S., Morimoto-Tomita, M., and Tomita, S. (2017). GARLH Family Proteins Stabilize GABAA Receptors at Synapses. Neuron *93*, 1138–1152.e6. https://doi.org/10.1016/j.neuron.2017.02.023.

43. Andiné, P., Jacobson, I., and Hagberg, H. (1988). Calcium uptake evoked by electrical stimulation is enhanced postischemically and precedes delayed neuronal death in CA1 of rat hippocampus: involvement of N-methyl-D-aspartate receptors. J. Cereb. Blood Flow Metab. *8*, 799–807. https://doi.org/10.1038/jcbfm.1988.135.

44. Kovalenko, T., Osadchenko, I., Nikonenko, A., Lushnikova, I., Voronin, K., Nikonenko, I., Muller, D., and Skibo, G. (2006). Ischemia-induced modifications in hippocampal CA1 stratum radiatum excitatory synapses. Hippocampus *16*, 814–825.

45. Congar, P., Gaïarsa, J.L., Popovici, T., Ben-Ari, Y., and Crépel, V. (2000). Permanent reduction of seizure threshold in post-ischemic CA3 pyramidal neurons. J. Neurophysiol. *83*, 2040–2046.

46. Saliba, R.S., Michels, G., Jacob, T.C., Pangalos, M.N., and Moss, S.J. (2007). Activity-dependent ubiquitination of GABA(A) receptors regulates their accumulation at synaptic sites. J. Neurosci. *27*, 13341–13351. https://doi.org/10.1523/JNEUROSCI.3277-07.2007.

47. Jin, H., Chiou, T.T., Serwanski, D.R., Miralles, C.P., Pinal, N., and De Blas, A.L. (2014). Ring finger protein 34 (RNF34) interacts with and

promotes gamma-aminobutyric acid type-A receptor degradation via ubiquitination of the gamma2 subunit. J. Biol. Chem. *289*, 29420–29436. https://doi.org/10.1074/jbc.M114.603068.

48. Liu, T., Li, H., Hong, W., and Han, W. (2016). Brefeldin A-inhibited guanine nucleotide exchange protein 3 is localized in lysosomes and regulates GABA signaling in hippocampal neurons. J. Neurochem. *139*, 748–756. https://doi.org/10.1111/jnc.13859.

49. Mele, M., Aspromonte, M.C., and Duarte, C.B. (2017). Downregulation of GABA(A) Receptor Recycling Mediated by HAP1 Contributes to Neuronal Death in In Vitro Brain Ischemia. Mol. Neurobiol. *54*, 45–57. https://doi.org/10.1007/s12035-015-9661-9.

50. Crosby, K.C., Gookin, S.E., Garcia, J.D., Hahm, K.M., Dell'Acqua, M.L., and Smith, K.R. (2019). Nanoscale Subsynaptic Domains Underlie the Organization of the Inhibitory Synapse. Cell Rep. *26*, 3284–3297.e3. https://doi.org/10.1016/j.celrep.2019.02.070.

51. Deng, G., Orfila, J.E., Dietz, R.M., Moreno-Garcia, M., Rodgers, K.M., Coultrap, S.J., Quillinan, N., Traystman, R.J., Bayer, K.U., and Herson, P.S. (2017). Autonomous CaMKII Activity as a Drug Target for Histological and Functional Neuroprotection after Resuscitation from Cardiac Arrest. Cell Rep. *18*, 1109–1117. https://doi.org/10.1016/j.celrep.2017.01.011.

STAR★METHODS

KEY RESOURCES TABLE

REAGENT or RESOURCE	SOURCE	IDENTIFIER
Antibodies		
GABA$_A$R-γ2 (imaging)	Synaptic Systems	Cat. #224 004; RRID: AB_10594245
GABA$_A$R-α1 (imaging)	Synaptic Systems	Cat. #224 203; RRID: AB_2232180
Anti-GFP (imaging)	ThermoFisher	Cat. #11122; RRID: AB_221569
Gephyrin (3B11; imaging)	Synaptic Systems	Cat. #147 111; RRID: AB_2619837
VGAT (rabbit; imaging)	Synaptic Systems	Cat. #131 003; RRID: AB_887869
LAMP1	Abcam	Cat. #24170; RRID: AB_775978
Anti-guinea pig Alexa Fluor - 568	Life Technologies	Cat. #11075; RRID: AB_141954
Anti-guinea pig Alexa Fluor - 647	Abcam	Cat. #150187; RRID: AB_2827756
Anti-mouse Alexa Fluor - 488	Life Technologies	Cat. #21202; RRID: AB_141607
Anti-rabbit Alexa Fluor - 488	Life Technologies	Cat. #21206; RRID: AB_2535792
Anti-rabbit Alexa Fluor - 647	Life Technologies	Cat. #31573; RRID: AB_2536183
GABA$_A$R-γ2 (WB)	NeuroMab	Cat. #75-442; RRID: AB_2566822
GABA$_A$R-α1 (WB)	NeuroMab	Cat. #75-136; RRID: AB_10697873
GABA$_A$R-β3 (WB)	NeuroMab	Cat. #75-149; RRID: AB_10673389
GABA$_A$R-β3 phospho-Ser408/409	Rockland	Cat. #612-401-D51; RRID: AB_11183444
GAPDH	GeneTex	Cat. #GTX627408; RRID: AB_11174761
GluA1 (AMPAR)	EMD Millipore	Cat. #ABN241; RRID: AB_2721164
HRP-conjugated goat anti-mouse	BioRad	Cat. #170-6516; RRID: AB_11125547
HRP-conjugated goat anti-rabbit	BioRad	Cat. #170-6515; RRID: AB_11125142
Chemicals, peptides, and recombinant proteins		
Cyclosporin A (CsA)	Tocris Bioscience	Cat. #1101
MDL-28170 (Calp-i)	Tocris Bioscience	Cat. #1146
Okadaic acid	Tocris Bioscience	Cat. #1136
Leupeptin	Tocris Bioscience	Cat. #1167
Pierce Sulfo-NHS-LC-Biotin	ThermoFisher	Cat. #PG82075
PLA mouse/rabbit kit	Sigma	Cat. #DUO92101
Pierce NeutrAvidin	ThermoFisher	Cat. #29201
QuantiTect Reverse Transcription Kit	Qiagen	Cat. #205311
QuantiTect SYBR Green PCR Kit	Qiagen	Cat. #204143
Experimental models: cell lines		
Primary hippocampal cultures	Smith Laboratory	N/A
Experimental models: organisms/strains		
Rat, Sprague Dawley Charles River	Charles River	RRID: RGD_734476
Mice, C57BL/6	Jackson Laboratory	RRID: IMSR_ORNL:C57BL-6-A-A
Oligonucleotides		
qGABRB3 F: GGGGTGTCCTTCTGGATCAATTA	Rajgor et al.[20]	N/A
qGABRB3 R: TCTCGAAGGTGAGTGTTGATG	Rajgor et al.[20]	N/A
qGABRG2 F: ACTTTACCATCCAGACCTACATTC	Rajgor et al.[20]	N/A
qGABRG2 R: GCAGGGACAGCATCCTTATT	Rajgor et al.[20]	N/A
qGAPDH F: GATGCTGGTGCTGAGTATGT	This paper	N/A

(Continued on next page)

Continued

REAGENT or RESOURCE	SOURCE	IDENTIFIER
qGAPDH R: GCTGACAATCTTGAGGGAGTT	This paper	N/A
Software and algorithms		
Prism 9	GraphPad	https://www.graphpad.com/scientific-software/prism/
ImageJ	NIH	https://imagej.nih.gov/ij/

RESOURCE AVAILABILITY

Lead contact

Any additional information or enquiries about reagents and resources should be directed to the Lead Contact, Katharine R. Smith (katharine.r.smith@cuanschutz.edu)

Materials availability

The transfer of plasmids generated for this study will be made available upon request. A payment and/or a completed Materials Transfer Agreement may be required.

Data and code availability

- Data: All data reported in this paper will be shared by the lead contact upon request.
- Code: This paper does not generate original code.
- Other items: Any additional information required to reanalyze the data reported in this paper is available from the lead contact upon request.

EXPERIMENTAL MODEL AND STUDY PARTICIPANT DETAILS

All animal procedures are in accordance with the National Institutes of Health (NIH) *Guide for the Care and Use of Laboratory Animals* and approved with the Institutional Animal Care and Use Committee at the University of Colorado, Denver Anschutz Medical Campus.

Dissociated hippocampal cultures

Primary neuronal cultures were prepared from dissected hippocampi of mixed sex neonatal rat pups (postnatal day 0-1) as previously described.[14,20,50] Hippocampal tissue was dissociated in papain and neurons were seeded in MEM containing 10% FBS and penicillin/streptomycin, either onto 18mm #1.5 glass coverslips at a density of 150,000-200,000 cells or 6-cm dishes at 3,000,000 cells. MEM was replaced 24h following plating with Neurobasal (NB) media (GIBCO) supplemented with B27 (GIBCO) and 2 mM Glutamax. Feedings were performed every 5 days by removing half the media and replacing with new NB media. Mitotic inhibitors were added at DIV5. Cultures were maintained at 37°C, 5% CO_2 for 15-18 DIV prior to experiments.

Cardiac arrest and cardiopulmonary resuscitation animal model

C57BL/6 mice (8-10 weeks old, both sexes) underwent cardiac arrest and cardiopulmonary resuscitation (CA/CPR) or sham surgeries as previously described (Deng et al., 2017). Mice were anesthetized (3% isoflurane), intubated and placed on a ventilator (160 breaths per min). Vitals were monitored by ECG and body temperature was maintained at 37.5°C $\pm$ 0.2°C. KCl injection via the jugular catheter induced asystolic CA for 6-7 min. CPR was induced by a slow injection of epinephrine (16μg epinephrine/ml, 0.9%saline), chest compression (~300/min) and ventilation of 100% O_2. If spontaneous recirculation was not achieved by 3-min of CPR, the animal was omitted from the experiments. Vitals were monitored up to 15 min following resuscitation, prior to harvesting samples.[27,51] Samples were collected immediately, or for reperfusion following CA/CPR, mice vitals were monitored following resuscitation before being removed from the ventilator. Mice recovered for 4 hours following CA/CPR injury before harvesting samples. Coronal sections were generated on a vibratome to micro-dissect CA1 and CA3 subregions of the hippocampus.

METHOD DETAILS

Oxygen glucose deprivation (OGD) treatments *in vitro*

DIV15-18 hippocampal neuronal cultures were exposed to OGD by applying a HEPES-buffered solution (25mM HEPES, pH 7.4, 140mM NaCl, 5mM KCl, 2mM $CaCl_2$, 1mM $MgCl_2$, and 10mM sucrose or supplemented with 10mM glucose for control). OGD-HEPES solution was placed in an anaerobic workstation at 37°C, 95% N_2 and 5% CO_2 (Bugbox Plus, Baker Co) 24-48 hours prior to treatments to allow deoxygenation. Neuronal cultures were washed twice and incubated with OGD-HEPES solution in the anoxic chamber prior to being harvested or fixed at specific timepoints as stated in each figure. Control neurons were incubated at 37°C, 5% CO_2 with Control-HEPES solution and harvested

or fixed at similar timepoints as OGD conditions. For reperfusion experiments, HEPES solution was replaced with conditioned media and placed in the aerobic incubator for specified time. Inhibitors were used at the following final concentration: Okadaic Acid – 0.5 μM or 50 nM; Cyclosporin A (CsA) – 5 μM; Calp-i – 100 μM; Leupeptin – 10 μM.

Immunocytochemistry (ICC)

Neuronal cultures on coverslips were fixed in 4% PFA solution (4% sucrose, 1X PBS and 50mM HEPES (pH 7.5)) for 5 min at RT and blocked in 5% BSA, 2% Normal Goat Serum (NGS) and 1X PBS at RT for 30 min. Surface GABA$_A$R-γ2 (1:500 Synaptic Systems Guinea Pig – 224004) staining was performed under nonpermeabilized conditions in blocking solution for 1 hour at RT. Coverslips were washed for 5 min (3X) in PBS followed by permeabilization in 0.5% NP-40 for two min and blocked at RT for 30 min. Gephyrin 3B11 (1:600 Synaptic Systems Mouse – 147111) and VGAT (1:1000 Synaptic Systems Rabbit - 131003) staining was performed in blocking solution for 1 hour followed by 5 min washes (3X). Coverslips were incubated with appropriate secondary antibodies (1:1000 ThermoFisher Alexa –Fluor 488, 568 and 647) for 1 hr in blocking solution. Coverslips were washed for 5 min (3X) before being mounted on microscope slides with ProLong Gold mounting media (Thermofisher).

Proximity Ligation Assay (PLA)

PLA was performed using the DuoLink *in situ* red PLA mouse/rabbit kit (Sigma) under permeabilized conditions. The GABA$_A$R-α1 subunit (1:500 Synaptic Systems Rabbit - 224203) and gephyrin (1:500 Synaptic Systems Mouse - 147011) antibodies were used at the same dilution as with ICC. PLA positive puncta reactivity was imaged by confocal microscopy (see below) and measured as density per 10μm in ImageJ.

Antibody feeding assay

Hippocampal cultures were live-labeled in conditioned media against an epitope that recognizes the extracellular N-terminal domain of surface GABA$_A$Rs (γ2) at a dilution of 1:150 for 25 minutes. Neurons were washed in prewarmed, sterile PBS (2X) before being replaced with conditioned media. Neurons were subject to control or OGD treatments and fixed with 4% PFA at different timepoints, unless reperfusion was performed. In the case of reperfusion, neurons were fixed at a specified time point after conditioned media was replaced. To saturate primary antibody against GABA$_A$R subunits still present at the surface, fixed neurons were incubated with a secondary antibody at a supersaturating dilution of 1:150 overnight at 4°C. Neurons were then rinsed once with PBS and immediately fixed again with 4% PFA for 10 minutes followed by PBS washes (3X). Cells were permeabilized for 2-3 minutes with 0.5% NP40 and blocked with 5% BSA + 2% NGS for 25 minutes before labeling internalized receptors with a secondary antibody conjugated to a different fluorophore at a dilution of 1:1000 for 1 hour at RT (e.g., Surface: anti-guinea pig-Alexa568; Internalized: anti-guinea pig-Alexa647). If staining for other intracellular endogenous proteins such as LAMP1 (1:500), a primary antibody step is undertaken as described in ICC section before the secondary against internal pools is applied. Neurons were washed in PBS for 10 minutes (3X) before mounting with Prolong Gold on coverslips.

Image acquisition and analysis

Confocal images were acquired on a Zeiss Axio Observer.Z1 upright microscope equipped with a Yokogawa CSU-X1 spinning disk unit; a 63X oil immersion objective (Plan-Apo/1.4 NA); an Evolve 512 EM-CCD camera (Photometrics) with 16-bit range; and SlideBook 6.0. Images were attained at 0.3 μm intervals (4μm Z-stack projection). Cluster analysis was performed using ImageJ (NIH) by selecting dendritic regions of interest (ROIs). A user-based threshold was determined by sampling several images per condition across all conditions and clusters were defined as a minimum size of 0.05μm^2. For *in vitro* experiments, ROIs were delineated by tracing along dendrites or around the soma. Density was calculated by measuring the length of dendrites analyzed (per 10μm) or the area of the soma (per μm^2). To calculate the Internalization Index, we divided the mean florescence intensity of the internalized receptor pool by the total mean florescence (internalized florescence + surface florescence). For colocalization experiments, a Pearson's coefficient was calculated in ImageJ using the Coloc2 plug-in to compared LAMP1 staining with internalized receptor florescence intensity (Threshold Regression: Costes, PSF: 3.0, Costes Randomization: 50). Three independent experiments analyzed 10-12 neurons per condition for a total of 30-36 neurons. All confocal imaging analysis was performed blind to experimental condition.

Surface biotinylation

As previously described,[14,40] hippocampal cultures were placed on ice to block the endocytic machinery and treated with biotin (Pierce) at 0.5mg/mL (in PBS+1mM CaCl$_2$+1mM MgCl$_2$) for 15 min. Neurons were quenched with BSA (1mg/mL) in PBS+ CaCl$_2$+ MgCl$_2$ solution for 15 min; harvested in RIPA buffer (50mM Tris pH 7.5, 1mM EDTA, 2mM EGTA, 150mM NaCl, 1% NP-40, 0.5% DOC, 0.1% SDS, 50mM NaF, 1mM Na$_3$VO$_4$ and protease inhibitor (Complete Mini, EDTA-free, Roche)); and permeabilized for 1 hour. Debris was pelleted at 4°C at 15,000 rpm for 10 min. 10% of the supernatant was collected for the total protein input and the remainder was incubated with 25 μl Ultralink Immobilized NeutrAvidin 50% slurry (Pierce) for 2 hours at 4°C. Beads were washed 3X with high salt RIPA (350mM NaCl) and analyzed by western blotting. The surface levels were normalized to the 10% input of total protein.

Western blotting

Cell lysates were harvested in RIPA buffer (see above) with protease inhibitor (Roche) and phosphatase inhibitor cocktail 3 (Sigma). Samples were solubilized for 20 mins and centrifuged at max speed for 10 mins. Samples were denatured with a 4X sample buffer (62.5mM Tris pH 6.8, 2% SDS, 25% glycerol, 0.01% Bromophenol Blue and 10% beta-2-mercaptoethanol) and heated at 95°C for 5 mins. Protein lysates were resolved on a 10% SDS-PAGE gel and transferred to PVDF membrane in a wet apparatus. Blots were blocked in either 5% milk (TBS-T) or 5% BSA (TBS-T) for phospho-specific antibodies and probed with primary antibody overnight at 4°C with the following: GABA$_A$R-β3 (1:5000 Neuromab 75149), GABA$_A$R-γ2 (1:1000 Neuromab 75442), GABA$_A$R-α1 (1:2000 Neuromab 75136), GABA$_A$R-β3 phospho-Ser408/409 (1:1000 Rockland 612-401-D51) and GAPDH (1:40,000 GeneTex 627408). Blots were washed for 10-min (3X) followed by incubation with secondary HRP-conjugated antibodies (1:10,000 Millipore) at room temperature for 1 hour. ECL western blotting substrates were used to visualize protein bands and densitometry measurements were performed in ImageJ. Total protein was normalized to GAPDH from the same gel. Phosphorylation levels were normalized to total protein levels from the same gel.

RNA isolation and RT-qPCR

RNA isolation was performed by harvesting hippocampal neuronal cultures in 200μL TRIZOL and precipitating RNA using standard techniques.[20] Once isolated, a cDNA library was generated through a reverse transcription reaction using a QuantiTect RT Kit (Qiagen). To quantify total mRNA levels, qPCRs were performed with the QuantiTect SYBR Green PCR Kit (Qiagen) on a BioRad CFX384 real time qPCR system by diluting the cDNA (1:10) into RNAase free water and using 1μL of mixture per reaction combined with a gene specific primer (see[20] for details). All qPCR readings were normalized to both GAPDH and 18S, which are broadly used housekeeping genes. qPCR cycling parameters were as follows: 95°C 15min, 94°C 15sec 55°C 30sec, 72°C 30sec for 40 cycles.

QUANTIFICATION AND STATISTICAL ANALYSIS

All statistical tests were performed in Prism7 (GraphPad) using t test or ANOVA, Bonferroni *post hoc* test. All experiments were performed at least 3 times (3 independent cultures or animals). The exact number of repeats and statistical details of experiments can be found in the figure legends. P values were considered significant if < 0.05. Bar graphs are displayed as mean ± SEM.